Title

The activity of cGMP-dependent protein kinase Iα is not directly regulated by oxidation-induced disulfide formation at cysteine 43

Journal

Journal of Biological Chemistry, 292(20)

ISSN

0021-9258

Authors

Kalyanaraman, Hema
Zhuang, Shunhui
Pilz, Renate B
et al.

Publication Date

2017-05-01

DOI

10.1074/jbc.c117.787358

Peer reviewed

The activity of cGMP-dependent protein kinase Iα is not directly regulated by oxidation-induced disulfide formation at cysteine 43

Received for publication, March 20, 2017, and in revised form, March 28, 2017 Published, Papers in Press, March 30, 2017, DOI 10.1074/jbc.C117.787358

Hema Kalyanaraman, Shunhui Zhuang, Renate B. Pilz, and Darren E. Casteel[1]

From the Department of Medicine, University of California, San Diego, La Jolla, California 92093

Edited by Henrik G. Dohlman

The type I cGMP-dependent protein kinases (PKGs) are key regulators of smooth muscle tone, cardiac hypertrophy, and other physiological processes. The two isoforms PKGIα and PKGIβ are thought to have unique functions because of their tissue-specific expression, different cGMP affinities, and isoform-specific protein-protein interactions. Recently, a non-canonical pathway of PKGIα activation has been proposed, in which PKGIα is activated in a cGMP-independent fashion via oxidation of Cys^{43}, resulting in disulfide formation within the PKGIα N-terminal dimerization domain. A "redox-dead" knock-in mouse containing a C43S mutation exhibits phenotypes consistent with decreased PKGIα signaling, but the detailed mechanism of oxidation-induced PKGIα activation is unknown. Therefore, we examined oxidation-induced activation of PKGIα, and in contrast to previous findings, we observed that disulfide formation at Cys^{43} does not directly activate PKGIα *in vitro* or in intact cells. In transfected cells, phosphorylation of Ras homolog gene family member A (RhoA) and vasodilator-stimulated phosphoprotein was increased in response to 8-CPT-cGMP treatment, but not when disulfide formation in PKGIα was induced by H_2O_2. Using purified enzymes, we found that the Cys^{43} oxidation had no effect on basal kinase activity or K_m and V_{max} values; however, PKGIα containing the C43S mutation was less responsive to cGMP-induced activation. This reduction in cGMP affinity may in part explain the PKGIα loss-of-function phenotype of the C43S knock-in mouse. In conclusion, disulfide formation at Cys^{43} does not directly activate PKGIα, and the C43S-mutant PKGIα has a higher K_a for cGMP. Our results highlight that mutant enzymes should be carefully biochemically characterized before making *in vivo* inferences.

The type I cGMP-dependent protein kinases play key roles in regulating vascular tone, intestinal motility, memory formation, and nociception in the spinal cord (1). The kinases are activated by cGMP, and cellular cGMP levels are increased by the activity of soluble and particulate guanylate cyclases, which are activated by nitric oxide or small peptides, respectively. Conversely, cellular cGMP levels are decreased by phosphodiesterases. Pharmacological cGMP-elevating agents include nitric-oxide donors (nitroglycerin, nitroprusside), direct guanylate cyclase activators (riociguat), and phosphodiesterase inhibitors (sildenafil, tadalafil). These agents are used clinically to treat cardiac ischemia, systemic and pulmonary hypertension, and erectile dysfunction (2).

The type I PKG gene produces splice variants (PKGIα and PKGIβ)[2] that differ in their first ~100 amino acids (3). The kinases have a similar domain structure, which can be roughly divided into N-terminal regulatory and C-terminal catalytic domains. The regulatory domain contains a number of functional subdomains. At the extreme N termini, leucine/isoleucine zippers (LZs) mediate homodimerization and facilitate binding to specific interacting proteins (4–9). After the LZs, each isoform has a unique autoinhibitory (AI) loop containing an inhibitory sequence that binds within the catalytic cleft and blocks substrate access in the absence of cGMP. The LZ and AI domains differ between PKGIα and PKGIβ. Next come two tandem cyclic nucleotide-binding domains (cNBD-A and cNBD-B) that have preferences for binding cGMP over cAMP (~2.4-fold higher for cNBD-A and ~240-fold for cNBD-B (10)). The catalytic domain has an N-terminal ATP-binding lobe and a C-terminal substrate recognition lobe, and the catalytic cleft is located in the crevice between these two lobes. In the canonical PKG activation pathway, cGMP binding to the cNBDs induces a conformational change in the regulatory domain that pulls the AI loop from the catalytic cleft, thereby activating the kinase by allowing substrate access to the catalytic center.

In addition to the canonical activation pathway, PKGIα has been reported to be directly activated by oxidation. In an earlier paper, Landgraf *et al.* (11) showed that metal-induced disulfide bond formation between Cys^{118}–Cys^{196} and/or Cys^{313}–Cys^{519} increased basal kinase activity to ~70% of the maximum activity that could be achieved with saturating amounts of cGMP.[3] More recently, Burgoyne *et al.* (12) demonstrated that disulfide-bond formation at Cys^{43}, which lies at the C-terminal

This work was supported in part by National Institutes of Health Grant RO1-HL132141 (to R. B. P.) and the University of California, San Diego, Department of Medicine (to D. E. C.). The authors declare that they have no conflicts of interest with the contents of this article. The content is solely the responsibility of the authors and does not necessarily represent the official views of the National Institutes of Health.

This article contains supplemental Fig. S1.

[1] To whom correspondence should be addressed: Dept. of Medicine, University of California, San Diego, 9500 Gilman Dr., La Jolla, CA 92093-0652. Tel.: 858-534-8806; Fax: 858-534-1421; E-mail: dcasteel@ucsd.edu.

[2] The abbreviations used are: PKG, cGMP-dependent protein kinase; LZ, leucine/isoleucine zipper; AI, autoinhibitory; VASP, vasodilator-stimulated phosphoprotein.

[3] In this manuscript, we number PKGIα residues starting with the initial methionine.

end of the PKGIα LZ, activated the kinase in a cGMP-independent manner. Although PKG dimer formation is stably mediated by the LZ, Cys[43] oxidation and disulfide formation cause the two peptide chains in the dimer to become covalently linked. In addition to direct kinase activation, Cys[43] oxidation has been proposed to alter the K_m and V_{max} for substrates and to increase PKGIα binding to specific interacting proteins (12). A knock-in mouse containing a "redox-dead" C43S-mutant PKGIα shows phenotypes consistent with a loss of PKGIα signaling (13–19), and these results have been used to argue for a predominant role for Cys[43] oxidation in PKGIα regulation. However, the enzymatic properties of the C43S mutant PKGIα were not thoroughly investigated.

Exactly how Cys[43] oxidation activates PKGIα is unknown. To explore the underlying mechanism, we began by comparing the activity of wild-type and C43S-mutant PKGIα under reducing and oxidizing conditions. Surprisingly, and in contrast to previous findings, we found that wild-type PKGIα activity was not directly increased by disulfide formation at Cys[43] and that Cys[43] oxidation had no effect on substrate phosphorylation. In addition, we found that the C43S mutation caused PKGIα to have a lower sensitivity to cGMP-induced activation.

Results

Oxidation-induced PKGIα dimerization does not lead to increased kinase activity in intact cells

In the original report describing activation of PKGIα by Cys[43] oxidation, A10 cells were transfected with wild-type or C43S-mutant PKGIα and treated with H_2O_2, and myosin light chain phosphorylation was examined (12). H_2O_2 treatment caused increased PKGIα disulfide bond formation in wild-type but not C43S-mutant PKGIα, and disulfide bond formation was correlated with decreased myosin light chain phosphorylation, presumably through PKGIα-induced activation of myosin phosphatase (5). Using a similar rationale, we examined whether PKGIα Cys[43] oxidation led to increased phosphorylation of known PKGIα substrates in cells. We transfected 293T cells with expression constructs for RhoA together with wild-type or C43S-mutant PKGIα and treated cells with 8-CPT-cGMP or H_2O_2. 8-CPT-cGMP-treated cells showed robust RhoA phosphorylation with both wild-type and C43S-mutant PKGIα (Fig. 1*A*, *top panel*, compare *lanes 1* and *2* and compare *lane 4* and *5*). As expected, treatment with H_2O_2 caused a pronounced increase in disulfide bond formation in wild-type but not C43S-mutant PKGIα (shown by gel shift under non-reducing conditions; Fig. 1*A*, *bottom panel*, compare *lanes 1* and *3* and compare *lanes 4* and *6*). Unexpectedly, H_2O_2 treatment had no effect on RhoA phosphorylation (Fig. 1*A*, *top panel*, compare *lanes 1* and *3*). Similar results were seen when vasodilator-stimulated phosphoprotein (VASP) phosphorylation was examined. PKG phosphorylates VASP at Ser[157] and Ser[239], and phosphorylation at Ser[157] causes VASP to migrate with a higher apparent molecular weight. Upon Western blotting of transfected cells probed with a VASP Ser(P)[239] antibody, VASP runs as a doublet, and 8-CPT-cGMP treatment causes VASP to completely shift to the upper band, indicating double phosphorylation of Ser[157] and Ser[239] (Fig. 1*B*, compare *lanes 1* and *2* and compare *lanes 4* and *5*). However, in H_2O_2-treated cells, there is only a slight shift in VASP migration, and this shift is seen in cells transfected with wild-type or C43S-mutant PKGIα, indicating that it is not due to Cys[43] oxidation (Fig. 1*B*, compare *lanes 1* and *3* and *lanes 4* and *6*). These results strongly suggest that Cys[43] disulfide bond formation does not activate PKGIα in cells.

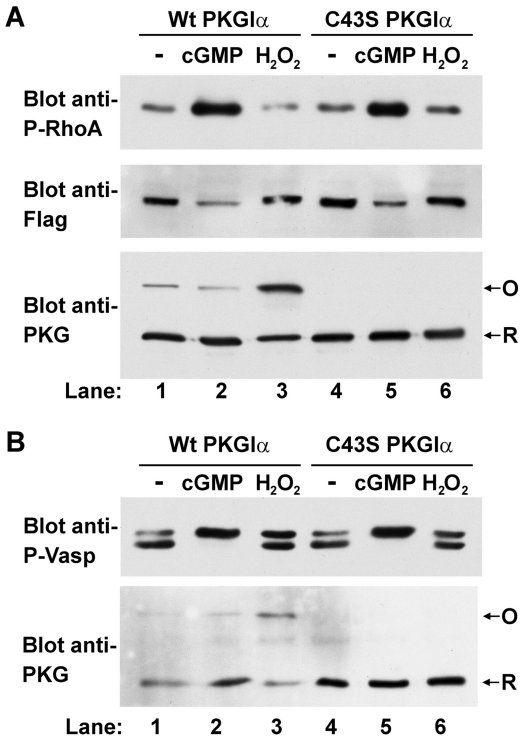

Figure 1. PKGIα is not activated in intact cells by disulfide formation at Cys[43]. *A*, 293T cells were transfected with expression vectors for Flag-tagged RhoA (500 ng) and untagged wild-type or C43S-mutant PKGIα (500 ng). The cells were treated for 60 min with 250 μM 8-CPT-cGMP, 100 μM H_2O_2, or vehicle alone, as indicated. RhoA Ser[188] phosphorylation was determined by SDS-PAGE under non-reducing conditions followed by immunoblotting with a RhoA Ser(P)[188] specific antibody. The amount of monomeric reduced (*R*) and disulfide-linked oxidized (*O*) PKGIα was determined by blotting with a PKGI specific antibody. *B*, performed as in *A*, except 293T cells were transfected with expression vectors for VSV-tagged VASP (200 ng) and wild-type or C43S-mutant PKGIα (200 ng), and blots were probed for VASP Ser(P)[239]. These experiments were repeated at least three times with similar results.

Oxidation of PKGIα Cys[43] does not increase kinase activity in vitro

To directly examine whether disulfide formation at Cys[43] increases kinase activity, we performed *in vitro* kinase assays. We used anti-Flag affinity beads to purify Flag-tagged PKGIα from transiently transfected 293T cells; this one-step purification protocol allowed us to quickly isolate highly purified full-length wild-type and C43S-mutant PKGIα (Fig. 2*A*). The purified kinases were incubated for 1 h in 15 mM DTT or allowed to oxidize by exposure to air in the absence of DTT. Immediately prior to measuring kinase activity, aliquots were removed for analysis by non-reducing SDS-PAGE/immunoblotting (as seen in Fig. 2*B*); under these conditions wild-type PKGIα was ~3.8% oxidized in the presence of DTT and ~59.7% oxidized in the absence of reducing agent. As expected, C43S-mutant PKGIα did not form a disulfide bond and ran as a monomer under both

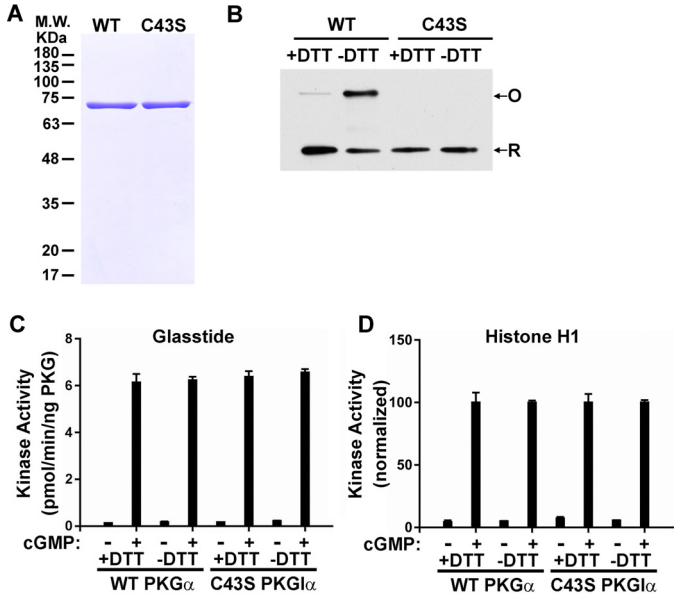

Figure 2. Cys[43] oxidation does not activate PKGIα *in vitro*. *A*, Coomassie-stained gel demonstrating the purity and integrity of Flag-tagged wild-type and C43S-mutant PKGIα isolated from transiently transfected 293T cells. *B*, purified wild-type and C43S mutant PKGIα were incubated in the presence or absence of 15 mM DTT and exposed to air for 1 h; the amount of Cys[43]-cross-linked PKGIα dimer was determined by non-reducing SDS-PAGE/immunoblotting. *C* and *D*, *in vitro* kinase assays were performed in the presence or absence of 10 μM cGMP using either Glasstide (*C*) or histone H1 (*D*) as substrates. Reactions were performed in triplicate from single protein preparations.

reducing and oxidizing conditions. Kinase assays performed using the small peptide Glasstide as a substrate revealed that oxidation slightly increased the basal activity of both wild-type and C43S-mutant PKGIα (Fig. 2*C*); basal activity of wild-type PKGIα increased from 0.137 to 0.206 pmol/min/μg, whereas activity of the C43S-mutant kinase increased from 0.170 to 0.214 pmol/min/μg (maximum kinase activity in the presence of cGMP was ~6.2 pmol/min/μg under all conditions). Identical results were found using Kemptide as a substrate (supplemental Fig. S1). It was recently reported that PKGIα Cys[43] disulfide bond formation increased *in vitro* PKGIα activity toward histone H1 but not RhoA (16). However, in contrast to those results, we found that Cys[43] oxidation did not increase PKGIα activity toward histone H1 (Fig. 2*D*); in fact, we did not even observe the slight oxidation-induced increase in basal activity of wild-type and mutant enzyme seen with small peptide substrates. Thus, under our conditions, oxidation of Cys[43] did not directly activate PKGIα *in vitro*.

PKGIα substrate affinity is not altered by oxidation at Cys[43]

PKGIα Cys[43] oxidation has been reported to change the enzyme kinetics (12). In previous studies, Burgoyne *et al.* (12) found that in the absence of cGMP, oxidation decreased the K_m for Glasstide from 247 to 37 μM but had no apparent effect on V_{max}, whereas in the presence of cGMP, oxidation lowered the K_m for Glasstide from 289 to 89 μM and lowered V_{max} by ~60% compared with the reduced enzyme. Because we found that oxidation did not directly activate PKGIα, we next examined whether oxidation altered PKGIα affinity for peptide substrates. Using purified wild-type and C43S-mutant PKGIα, we performed *in vitro* kinase assays under the same oxidizing or reducing conditions described above. In the presence of cGMP, we found that oxidation/reduction caused no difference in the K_m or V_{max} for Glasstide in wild-type or C43S-mutant PKGIα (Fig. 3, *A* and *B*). In the absence of cGMP, oxidation slightly increased V_{max} in both wild-type and C43S-mutant PKGIα (note the different scales in Fig. 3). This slight increase in basal activity was similar to what was seen in Fig. 2*C* and was not due to disulfide bond formation at Cys[43], because it was the same in wild-type and C43S-mutant enzyme. The complete set of K_m and V_{max} values are listed in Table 1. Fig. 3*E* shows the amount of reduced *versus* Cys[43]-cross-linked PKGIα for each reaction condition.

PKGIα C43S has a reduced affinity for cGMP

We next checked whether oxidation altered the response of PKGIα to cGMP. Using wild-type and C43S-mutant PKGIα under oxidizing and reducing conditions, we performed *in vitro* kinase assays in the presence of increasing amounts of cGMP (Fig. 4). We found that oxidation of wild-type PKGIα had no significant effect on the K_a for cGMP: K_a = 0.074 ± 0.003 and 0.072 ± 0.004 μM for the reduced and oxidized wild-type enzyme, respectively. However, unexpectedly, we found that the C43S mutation caused PKGIα to require a higher amount of cGMP to half-maximally activate the kinase: K_a = 0.373 ± 0.017 and 0.337 ± 0.015 μM for the reduced and oxidized mutant enzyme, respectively. Thus, whereas reduction/oxidation had no effect on cGMP-induced activation of wild-type or C43S-mutant PKGIα, the C43S mutation caused PKGIα to be less sensitive to activation by cGMP.

Taken together, our results demonstrate that PKGIα is not directly activated by Cys[43] oxidation, and Cys[43] oxidation does not change the kinetic properties of the enzyme toward substrates. However, the C43S mutation causes an ~5-fold decrease in cGMP affinity of the enzyme. This loss in cGMP sensitivity could explain the reported phenotype of the C43S knock-in mouse, which appears to have a loss of PKGIα function.

Discussion

Since its discovery in the 1970s, PKG has been extensively studied; however, some of its biochemical properties are still incompletely defined. Recent structural studies have demonstrated unique features that play important roles in regulating cGMP-induced kinase activity, including the structural basis for cGMP selectivity and novel interchain contacts that regulate kinase activation (10, 20, 21). Another recently proposed mechanism for PKGIα regulation was direct activation by oxidation-induced disulfide bond formation at Cys[43]. How the formation of a disulfide bond at Cys[43] activates the kinase was not determined, and investigating the mechanism was the starting point for our current study.

In contrast to previous reports, we found that oxidation of PKGIα at Cys[43] does not directly activate PKGIα. In addition, Cys[43] oxidation had no effect on substrate affinity or reaction velocity using Glasstide as a substrate, and oxidation did not lead to increased histone H1 phosphorylation. Although it is unclear why our results differ from earlier studies, one factor

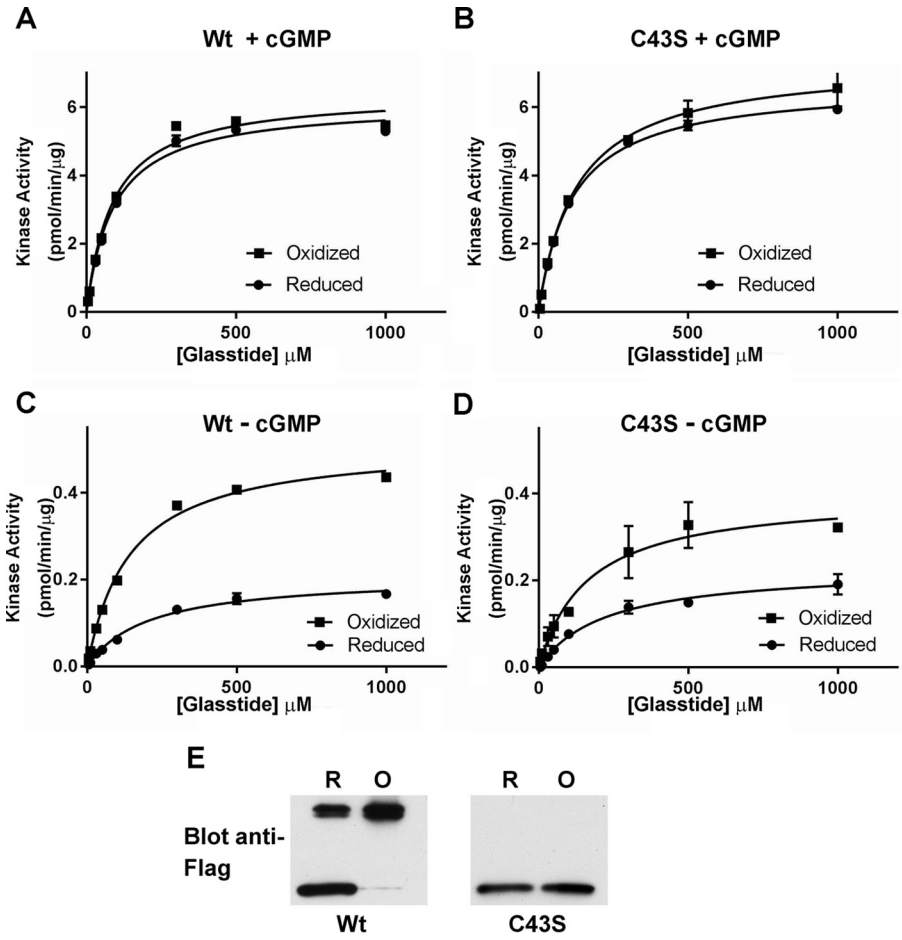

Figure 3. Wild-type and C43S-mutant PKGIα enzyme kinetics. *A*, PKGIα was incubated in the presence or absence of 15 mM DTT for 1 h, and kinase assays were performed in the presence of 10 μM cGMP and increasing amounts of Glasstide. *B*, C43S PKGIα was incubated in the presence or absence of 15 mM DTT for 1 h, and kinase assays were performed as described in *A*. *C*, PKGIα activity was measured as in *A*, but in the absence of cGMP. *D*, C43S-mutant PKGIα activity was measured as in *B*, without cGMP. Reactions were performed in triplicate from single protein preparations, and repeated with two independent protein preps. *E*, Western blot showing relative amount of reduced (*R*) and Cys^{43} oxidized (*O*) PKGIα in the kinase samples used for the reactions. V_{max} and K_m values were calculated using GraphPad Prism 7.

Table 1

Summary of kinetic constants toward Glasstide for wild-type and C43S-mutant PKGIα under oxidizing and reducing conditions

	K_m	V_{max}
	μM	*pmol/min/μg*
Reduced wild type + cGMP	89.9 ± 5.5	6.1 ± 0.1
Oxidized wild type + cGMP	87.8 ± 3.1	6.4 ± 0.1
Reduced C43S mutant + cGMP	113.5 ± 3.9	6.7 ± 0.1
Oxidized C43S mutant + cGMP	128.3 ± 8.3	7.3 ± 0.1
Reduced wild type − cGMP	202.8 ± 19.5	0.209 ± 0.0
Oxidized wild type − cGMP	142.7 ± 7.7	0.514 ± 0.0
Reduced C43S mutant − cGMP	221.9 ± 28.9	0.229 ± 0.0
Oxidized C43S mutant − cGMP	161 ± 30.5	0.397 ± 0.0

may be that the original studies were performed using PKGIα purchased from a commercial vendor and that the kinase could only be stimulated 1.5–3-fold by cGMP (12). This suggests that the kinase was proteolytically degraded, leading to a largely cGMP-independent kinase activity, and the poor quality of the enzyme may have affected the biochemical assays. In a subsequent paper by Prysyazhna *et al.* (16), PKGIα was purified using a cAMP-agarose affinity column, followed by cAMP elution and dialysis to remove cAMP. This kinase could be stimulated ~8-fold by cGMP as determined by Western blotting performed with phospho-specific antibodies to detect RhoA and histone H1 phosphorylation (see Fig. 6*A* in Ref. 16). In our experience, it is very difficult to fully remove cAMP during PKG purification, especially from PKGIα (10, 20, 22), and in general, Western blotting is semi-quantitative and is not an accurate method to measure kinase activity.

It could be argued that the N-terminal Flag tag on our PKGIα constructs affected kinase activity; however, we note that the kinase used in the present studies was purified intact, had a low basal activity, and could be stimulated 20–50-fold by cGMP. In addition, the Flag-tagged wild-type kinase had a K_a for cGMP of 72–74 μM, which is consistent with previous results measuring the K_a of untagged PKGIα in cell lysates (23, 24). Our V_{max} and K_m values for Glasstide differ from those obtained by Glass and Krebs (K_m = 28.8 μM and V_{max} = 20 pmol/min/μg (25)); the different values may reflect the variation in kinase assay conditions, because their assays were performed using 2 mM Mg^{2+}, whereas we used 10 mM Mg^{2+}. In addition, Glass and Krebs had found that for small peptide substrates, PKGIα activity peaked at 2 mM Mg^{2+} and rapidly decreased as free Mg^{2+} levels increased, whereas for large substrates like histone, activity steadily increased as free Mg^{2+} reached 75 mM (26). In comparison with our assays, previous *in vitro* kinase assays determining

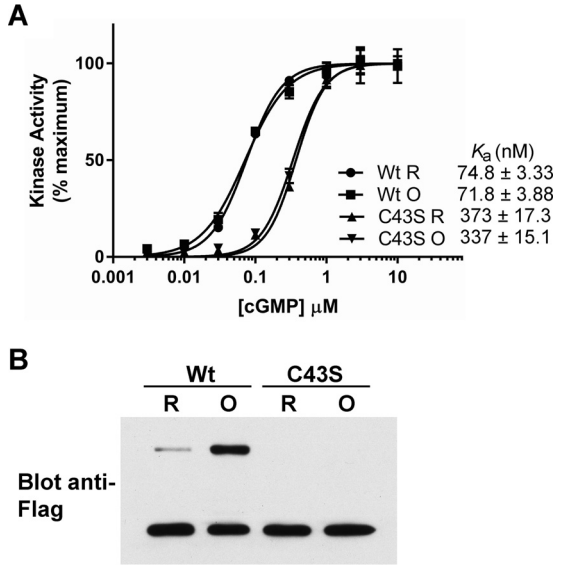

Figure 4. C43S-mutant PKGIα has a decreased affinity for cGMP. *A*, purified Flag-tagged wild-type and C43S-mutant PKGIα were incubated in the presence or absence of 15 mM DTT, exposed to air for 1 h, and used in *in vitro* kinase reactions with 500 μM Glasstide as a substrate and increasing amounts of cGMP. *Numbers* are the averages of four values from two independent protein preparations, with reactions performed in duplicate. K_a values were calculated using GraphPad Prism 7. *B*, Western blot showing relative amount of reduced (*R*) and oxidized (*O*) PKG in the kinase samples used for the reactions.

the effects of Cys[43] oxidation were performed with either 5 or 15 mM $MgCl^{2+}$ (12, 16). We should also point out that the transfected kinases used for our in-cell assays were without epitope tag (Fig. 1), demonstrating that oxidation did not increase the activity of untagged PKGIα in cells. Therefore, we do not feel that the N-terminal Flag tag affected our results.

We found that C43S-mutant PKGIα has an ~5-fold lower affinity for cGMP compared with the wild-type enzyme. This is an important finding, because mice homozygous for C43S-mutant PKGIα have phenotypes consistent with a loss of PKGIα function (17–19). These phenotypes include hypertension, insensitivity to nitroglycerin-induced vasodilation, and protection from septic shock; they have been interpreted to be the result of defective redox-sensing properties normally ascribed to Cys[43] disulfide bond formation. However, mice null for the β_1 subunit of soluble guanylate cyclase are also resistant to nitroglycerin-induced vasodilation (27), indicating that the canonical NO-cGMP-PKG pathway is important and that oxidation sensing by Cys[43] disulfide formation is not the main mechanism for nitroglycerin-induced vasodilation. Although our current studies have not looked at PKGIα oxidation in mice, our results strongly suggest that defective signaling in PKGIα C43S mice is due at least in part to an increased K_a for cGMP rather than a loss of redox-induced activation of the enzyme.

It is possible that loss of Cys[43] oxidation might also affect other aspects of PKGIα signaling; for example, oxidation of PKGIα may alter its interaction with specific interacting proteins, which have been shown to bind to the PKGIα leucine zipper (5, 7, 28). Indeed, oxidation has been shown to increase the *in vitro* interaction between PKGIα and two of its interacting proteins, RhoA and MYPT1 (12). In addition, a recent paper by Nakamura *et al.* (15) demonstrated that the C43S mutation appeared to alter PKGIα subcellular localization in cardiac myocytes, which suggests a change in association of with interacting/anchoring proteins in cells, but the structural basis for oxidation-induced changes in these interactions was not examined. We are currently pursuing these studies.

How does the C43S mutation lead to decreased cGMP affinity? Since PKGIα and PKGIβ were first purified, it has been known that their different N termini cause the two isoforms to have different K_a values for cGMP, even though the sequences of the cyclic-nucleotide-binding pockets are identical (23). We have previously used hydrogen/deuterium-exchange mass spectrometry to study the PKGIβ regulatory domain and found that, in the presence of the N-terminal LZ and autoinhibitory subdomains, hydrogen/deuterium exchange was increased throughout the cGMP-binding pockets (29). The increased conformational dynamics correlate with increased cGMP affinity. Because small molecule ligands are thought to stabilize preexisting protein conformations (30, 31), we reasoned that the N terminus shifted the ensemble of conformations that PKGIβ adopts in solution, such that the cyclic nucleotide-binding pockets spend more time in conformations that resemble the cGMP-bound forms. Therefore, it is possible that the C43S mutation, which lies at the end of the LZ, causes a change in the conformational dynamics of the nucleotide-binding pockets, which leads to lower cGMP affinity. In a previous analysis of the PKGIα LZ, the C43S mutation lowered the T_m for thermal denaturation from >108 to 81.4 °C under oxidizing conditions and from 93.0 to 83.3 °C under reducing conditions (32). Although these melting temperatures are not physiological, thermal denaturation measures melting of the entire LZ, and the lower T_m in the C43S-mutant samples may reflect structural destabilization of the region surrounding Cys[43], which could occur in the full-length protein under physiological conditions.

In conclusion, we found that disulfide formation at Cys[43] does not directly activate PKGIα *in vitro* or in intact cells. In addition, "redox dead" C43S-mutant PKGIα has a higher K_a for cGMP, and this decreased cGMP affinity may at least partially explain the loss-of-function PKGIα phenotype observed in the C43S knock-in mice. Our results also highlight the general fact that mutant enzymes should be carefully characterized biochemically before cellular or physiological inferences are made.

Experimental procedures

Antibodies and reagents

Antibodies specific for Ser(P)[188] of RhoA (sc-32954; lot no. A0914) and PKGIα/β (sc-25429; lot no. F0910) were from Santa Cruz Biotechnology. Anti-VASP Ser(P)[239] antibody was from Cell Signaling Technology (31145; lot no. 5). Anti-Flag M2 antibody F1804; lot no. 101M6216), anti-Flag M2 affinity gel, and Flag peptide were from Sigma. Horseradish-peroxidase-conjugated goat anti-mouse (115-035-062) and goat anti-rabbit (111-035-046) antibodies were from Jackson ImmunoResearch. Kemptide and Glasstide were from AnaSpec, Inc. Histone H1 (sc-221729; lot no. J2115) was from Santa Cruz Biotechnology.

General laboratory reagents were from Fisher Scientific, Sigma Life Science, or Bio-Rad.

DNA constructs

Expression vectors for untagged PKGIα, Flag-RhoA, and VSV-VASP have been described previously (33–35). The Flag-tagged expression vector pFlag-D was constructed by annealing the oligonucleotides 5′-AGCTGCCACCATGGACTACAAAGACGATGACGACAAGG-3′ (sense) and 5′-GATCCCTTGTCGTCATCGTCTTTGTAGTCCATGGTGG-3′ (antisense) and ligating them into HindIII/BamHI-cut pcDNA3. Flag-tagged PKGIα was generated by PCR using the following set of primers: 5′-GACGGATCCGCCGCCATGAGCGAGCTAGAGGAAG-3′ (sense) and 5′-GCACTCGAGTTATTAGAAGTCTATATCCCATCC-3′ (antisense). The PCR product was digested with BamHI/XhoI and ligated into BamHI/XhoI-cut pFlag-D. The C43S mutation in PKGIα was generated using overlapping extension PCR (36, 37), and the mutant PKGIα coding sequence was cut with BamHI/XhoI and ligated into BamHI/XhoI-cut pcDNA3 and pFlag-D to produce untagged and Flag-tagged expression vectors. All PCR-derived PKG constructs were sequenced.

Cell culture and transfection

293T cells were grown in Dulbecco's modified Eagle's medium supplemented with 10% fetal bovine serum at 37 °C in a 5% CO_2 atmosphere. The cells were transfected using Lipofectamine 2000 according to the manufacturer's instructions (Life Technologies).

RhoA and VASP phosphorylation in 293T cells and Western blotting

293T cells were split into 12-well cluster dishes such that they would be 90–95% confluent 18 h later, at the time of transfection. The cells were transfected with expression vectors for wild-type or C43S-mutant PKGIα and RhoA or VASP as indicated in the figure legends. The next day, the wells were treated for 60 min with 250 μM 8-CPT-cGMP, 100 μM H_2O_2, or vehicle as indicated. The medium was aspirated, and the cells were directly lysed by adding non-reducing SDS sample buffer (60 mM Tris-HCl, pH 6.8, 2% SDS, 0.01% bromphenol blue, and 100 mM maleimide (to prevent oxidation during sample processing)). Cell lysates were transferred to microcentrifuge tubes and sonicated 2 × 20 s at 1-watt power. The proteins were separated by SDS-PAGE, transferred to Immobilon-P, blocked in 5% nonfat dry milk in TBS, and blotted with the indicated antibodies. The blots were developed using SuperSignal West Pico Chemiluminescent Substrate (Thermo Scientific).

Protein expression and purification

The cells were split into a 6-well cluster dish and transfected with Flag-tagged wild-type or C43S PKGIα (three wells each). Approximately 20 h post-transfection, the cells were scraped in PBS and lysed in buffer A (PBS, 0.1% Nonidet P-40) containing 1× protease inhibitor mixture (Calbiochem), and lysates were cleared by centrifugation (16,000 × *g*, 10 min at 4 °C). Cleared lysates were incubated with 20 μl of anti-Flag M2 affinity gel (Sigma) for 1 h at 4 °C with constant mixing. The beads were washed 2 × 200 μl of buffer A, 2 × 200 μl of PBS with 500 mM NaCl, and 2 × 200 μl of PBS. Bound proteins were eluted with 4 × 10 μl of elution buffer (PBS with 100 μg/ml Flag peptide). For each elution step, the beads were incubated with buffer for 5 min on ice. The four eluates for each protein were pooled. Proteins were quantified by SDS-PAGE/Coomassie staining using BSA standards on the same gel. The gels were scanned, and quantification was performed using ImageJ.

Kinase oxidation/reduction and in vitro kinase assays

Flag-tagged wild-type and C43S PKGIα purified from transiently transfected 293T cells were diluted to ~1 ng/μl in kinase dilution buffer (10 mM potassium phosphate, pH 7.0, 1 mM EDTA, and 0.1% BSA). For reduced samples, the dilution buffer contained 15 mM DTT. 10 μl of diluted kinase was added to 5 μl of 3× kinase reaction mix (120 mM HEPES, pH 7.4, 1.5 mM Glasstide, 30 mM $MgCl_2$, 150 μM ATP, 180 μCi/ml [γ-^{32}P]ATP, and ± 30 μM cGMP). The reactions were performed for 1.5 min at 30 °C and stopped by spotting on P81 phosphocellulose paper. Unincorporated [γ-^{32}P]ATP was removed by washing P81 paper four times for 5 min with 2 liters of 0.452% *o*-phosphoric acid. ^{32}P incorporation was measured by liquid scintillation counting. In some experiments, 1.5 mM Glasstide was replaced by 1.56 mg/ml Kemptide or 3 μg of histone H1. The reactions with histone H1 were run for 8 min. For experiments examining enzyme kinetics, reactions were performed ± 10 μM cGMP with increasing amounts of Glasstide (0.005–1.0 μM) or with 1.5 mM Glasstide in the presence of increasing concentrations of cGMP (0.003–10 μM).

Data analysis

The data were analyzed using GraphPad Prism 7. The V_{max} and K_m values were measured using non-linear fit Michaelis-Menten analysis, and cGMP K_a values were determined by plotting [agonist] *versus* normalized response with variable slope.

Author contributions—D. E. C. conceived the project. H. K., S. Z., and D. E. C. performed the experiments. R. B. P. and D. E. C. analyzed the data and wrote the paper.

References

1. Ruth, P. (1999) Cyclic GMP-dependent protein kinases: understanding *in vivo* functions by gene targeting. *Pharmacol. Ther* **82,** 355–372
2. Hoffmann, L. S., and Chen, H. H. (2014) cGMP: transition from bench to bedside: a report of the 6th International Conference on cGMP Generators, Effectors and Therapeutic Implications. *Naunyn Schmiedebergs Arch. Pharmacol.* **387,** 707–718
3. Hofmann, F., Bernhard, D., Lukowski, R., and Weinmeister, P. (2009) cGMP regulated protein kinases (cGK). *Handb. Exp. Pharmacol.* 137–162
4. Schlossmann, J., Ammendola, A., Ashman, K., Zong, X., Huber, A., Neubauer, G., Wang, G. X., Allescher, H. D., Korth, M., Wilm, M., Hofmann, F., and Ruth, P. (2000) Regulation of intracellular calcium by a signalling complex of IRAG, IP3 receptor and cGMP kinase Iβ. *Nature* **404,** 197–201
5. Surks, H. K., Mochizuki, N., Kasai, Y., Georgescu, S. P., Tang, K. M., Ito, M., Lincoln, T. M., and Mendelsohn, M. E. (1999) Regulation of myosin phosphatase by a specific interaction with cGMP-dependent protein kinase Iα. *Science* **286,** 1583–1587
6. Takimoto, E., Koitabashi, N., Hsu, S., Ketner, E. A., Zhang, M., Nagayama, T., Bedja, D., Gabrielson, K. L., Blanton, R., Siderovski, D. P., Mendelsohn, M. E., and Kass, D. A. (2009) Regulator of G protein signaling 2 mediates

cardiac compensation to pressure overload and antihypertrophic effects of PDE5 inhibition in mice. *J. Clin. Invest.* **119,** 408–420
7. Kato, M., Blanton, R., Wang, G. R., Judson, T. J., Abe, Y., Myoishi, M., Karas, R. H., and Mendelsohn, M. E. (2012) Direct binding and regulation of RhoA protein by cyclic GMP-dependent protein kinase Iα. *J. Biol. Chem.* **287,** 41342–41351
8. Casteel, D. E., Zhuang, S., Gudi, T., Tang, J., Vuica, M., Desiderio, S., and Pilz, R. B. (2002) cGMP-dependent protein kinase Iβ physically and functionally interacts with the transcriptional regulator TFII-I. *J. Biol. Chem.* **277,** 32003–32014
9. Schwappacher, R., Rangaswami, H., Su-Yuo, J., Hassad, A., Spitler, R., and Casteel, D. E. (2013) cGMP-dependent protein kinase Iβ regulates breast cancer cell migration and invasion via interaction with the actin/myosin-associated protein caldesmon. *J. Cell Sci.* **126,** 1626–1636
10. Huang, G. Y., Kim, J. J., Reger, A. S., Lorenz, R., Moon, E. W., Zhao, C., Casteel, D. E., Bertinetti, D., Vanschouwen, B., Selvaratnam, R., Pflugrath, J. W., Sankaran, B., Melacini, G., Herberg, F. W., and Kim, C. (2014) Structural basis for cyclic-nucleotide selectivity and cGMP-selective activation of PKG I. *Structure* **22,** 116–124
11. Landgraf, W., Regulla, S., Meyer, H. E., and Hofmann, F. (1991) Oxidation of cysteines activates cGMP-dependent protein kinase. *J. Biol. Chem.* **266,** 16305–16311
12. Burgoyne, J. R., Madhani, M., Cuello, F., Charles, R. L., Brennan, J. P., Schröder, E., Browning, D. D., and Eaton, P. (2007) Cysteine redox sensor in PKGIa enables oxidant-induced activation. *Science* **317,** 1393–1397
13. Burgoyne, J. R., and Eaton, P. (2013) Detecting disulfide-bound complexes and the oxidative regulation of cyclic nucleotide-dependent protein kinases by H2O2. *Methods Enzymol.* **528,** 111–128
14. Lorenz, J. E., Kallenborn-Gerhardt, W., Lu, R., Syhr, K. M., Eaton, P., Geisslinger, G., and Schmidtko, A. (2014) Oxidant-induced activation of cGMP-dependent protein kinase Iα mediates neuropathic pain after peripheral nerve injury. *Antioxid. Redox Signal.* **21,** 1504–1515
15. Nakamura, T., Ranek, M. J., Lee, D. I., Shalkey Hahn, V., Kim, C., Eaton, P., and Kass, D. A. (2015) Prevention of PKG1α oxidation augments cardioprotection in the stressed heart. *J. Clin. Invest.* **125,** 2468–2472
16. Prysyazhna, O., Burgoyne, J. R., Scotcher, J., Grover, S., Kass, D., and Eaton, P. (2016) Phosphodiesterase 5 inhibition limits doxorubicin-induced heart failure by attenuating protein kinase G Iα oxidation. *J. Biol. Chem.* **291,** 17427–17436
17. Prysyazhna, O., Rudyk, O., and Eaton, P. (2012) Single atom substitution in mouse protein kinase G eliminates oxidant sensing to cause hypertension. *Nat. Med.* **18,** 286–290
18. Rudyk, O., Phinikaridou, A., Prysyazhna, O., Burgoyne, J. R., Botnar, R. M., and Eaton, P. (2013) Protein kinase G oxidation is a major cause of injury during sepsis. *Proc. Natl. Acad. Sci. U.S.A.* **110,** 9909–9913
19. Rudyk, O., Prysyazhna, O., Burgoyne, J. R., and Eaton, P. (2012) Nitroglycerin fails to lower blood pressure in redox-dead Cys42Ser PKG1α knock-in mouse. *Circulation* **126,** 287–295
20. Osborne, B. W., Wu, J., McFarland, C. J., Nickl, C. K., Sankaran, B., Casteel, D. E., Woods, V. L., Jr, Kornev, A. P., Taylor, S. S., and Dostmann, W. R. (2011) Crystal structure of cGMP-dependent protein kinase reveals novel site of interchain communication. *Structure* **19,** 1317–1327
21. Kim, J. J., Lorenz, R., Arold, S. T., Reger, A. S., Sankaran, B., Casteel, D. E., Herberg, F. W., and Kim, C. (2016) Crystal structure of PKG I:cGMP complex reveals a cGMP-mediated dimeric interface that facilitates cGMP-induced activation. *Structure* **24,** 710–720
22. Kim, J. J., Casteel, D. E., Huang, G., Kwon, T. H., Ren, R. K., Zwart, P., Headd, J. J., Brown, N. G., Chow, D. C., Palzkill, T., and Kim, C. (2011) Co-crystal structures of PKG Iβ (92–227) with cGMP and cAMP reveal the molecular details of cyclic-nucleotide binding. *PLoS One* **6,** e18413
23. Ruth, P., Landgraf, W., Keilbach, A., May, B., Egleme, C., and Hofmann, F. (1991) The activation of expressed cGMP-dependent protein kinase isozymes Iα and Iβ is determined by the different amino-termini. *Eur. J. Biochem.* **202,** 1339–1344
24. Ruth, P., Pfeifer, A., Kamm, S., Klatt, P., Dostmann, W. R., and Hofmann, F. (1997) Identification of the amino acid sequences responsible for high affinity activation of cGMP kinase Iα. *J. Biol. Chem.* **272,** 10522–10528
25. Glass, D. B., and Krebs, E. G. (1982) Phosphorylation by guanosine 3′:5′-monophosphate-dependent protein kinase of synthetic peptide analogs of a site phosphorylated in histone H2B. *J. Biol. Chem.* **257,** 1196–1200
26. Glass, D. B., and Krebs, E. G. (1979) Comparison of the substrate specificity of adenosine 3′:5′-monophosphate- and guanosine 3′:5′-monophosphate-dependent protein kinases. Kinetic studies using synthetic peptides corresponding to phosphorylation sites in histone H2B. *J. Biol. Chem.* **254,** 9728–9738
27. Friebe, A., Mergia, E., Dangel, O., Lange, A., and Koesling, D. (2007) Fatal gastrointestinal obstruction and hypertension in mice lacking nitric oxide-sensitive guanylyl cyclase. *Proc. Natl. Acad. Sci. U.S.A.* **104,** 7699–7704
28. Yuasa, K., Omori, K., and Yanaka, N. (2000) Binding and phosphorylation of a novel male germ cell-specific cGMP-dependent protein kinase-anchoring protein by cGMP-dependent protein kinase Iα. *J. Biol. Chem.* **275,** 4897–4905
29. Lee, J. H., Li, S., Liu, T., Hsu, S., Kim, C., Woods, V. L., Jr, and Casteel, D. E. (2011) The amino terminus of cGMP-dependent protein kinase Iβ increases the dynamics of the protein's cGMP-binding pockets. *Int. J. Mass Spectrom.* **302,** 44–52
30. Kern, D., and Zuiderweg, E. R. (2003) The role of dynamics in allosteric regulation. *Curr. Opin. Struct. Biol.* **13,** 748–757
31. Huang, Y. J., and Montelione, G. T. (2005) Structural biology: proteins flex to function. *Nature* **438,** 36–37
32. Qin, L., Reger, A. S., Guo, E., Yang, M. P., Zwart, P., Casteel, D. E., and Kim, C. (2015) Structures of cGMP-dependent protein kinase (PKG) Iα leucine zippers reveal an interchain disulfide bond important for dimer stability. *Biochemistry* **54,** 4419–4422
33. Casteel, D. E., Zhang, T., Zhuang, S., and Pilz, R. B. (2008) cGMP-dependent protein kinase anchoring by IRAG regulates its nuclear translocation and transcriptional activity. *Cell Signal.* **20,** 1392–1399
34. Zhuang, S., Nguyen, G. T., Chen, Y., Gudi, T., Eigenthaler, M., Jarchau, T., Walter, U., Boss, G. R., and Pilz, R. B. (2004) Vasodilator-stimulated phosphoprotein activation of serum-response element-dependent transcription occurs downstream of RhoA and is inhibited by cGMP-dependent protein kinase phosphorylation. *J. Biol. Chem.* **279,** 10397–10407
35. Casteel, D. E., Turner, S., Schwappacher, R., Rangaswami, H., Su-Yuo, J., Zhuang, S., Boss, G. R., and Pilz, R. B. (2012) Rho isoform-specific interaction with IQGAP1 promotes breast cancer cell proliferation and migration. *J. Biol. Chem.* **287,** 38367–38378
36. Higuchi, R., Krummel, B., and Saiki, R. K. (1988) A general method of in vitro preparation and specific mutagenesis of DNA fragments: study of protein and DNA interactions. *Nucleic Acids Res.* **16,** 7351–7367
37. Ho, S. N., Hunt, H. D., Horton, R. M., Pullen, J. K., and Pease, L. R. (1989) Site-directed mutagenesis by overlap extension using the polymerase chain reaction. *Gene* **77,** 51–59